

## N<sub>2</sub>O Decomposition

# Direct Decomposition of Nitrous Oxide to Nitrogen by In Situ Oxygen Removal with a Perovskite Membrane\*\*

Heqing Jiang, Haihui Wang,\* Fangyi Liang, Steffen Werth,\* Thomas Schiestel, and Jürgen Caro\*

Nitrous oxide (N<sub>2</sub>O) has recently received much attention as it greatly contributes to the greenhouse effect<sup>[1]</sup> and causes severe destruction of the ozone layer in the stratosphere.<sup>[2]</sup> N<sub>2</sub>O is produced by both natural and anthropogenic sources;<sup>[3–5]</sup> N<sub>2</sub>O emissions that can be reduced in the short term are associated with chemical and energy industries.<sup>[6,7]</sup> The major N<sub>2</sub>O emission of chemical production comes from adipic acid and nitric acid plants. In the past decades, significant efforts have been devoted to the development of technologies for N<sub>2</sub>O reduction. Possible methods include: 1) non-selective catalytic reduction (NSCR), 2) selective catalytic reduction (SCR), and 3) catalytic decomposition of N<sub>2</sub>O to O<sub>2</sub> and N<sub>2</sub>. NSCR has been developed for NO<sub>x</sub> removal and has shown potential for reducing N<sub>2</sub>O. However, NSCR is not the optimum choice because of high secondary emissions of CO<sub>x</sub> and high cost of the reductant.<sup>[8,9]</sup> SCR of N<sub>2</sub>O with hydrocarbons has been extensively investigated over iron-based zeolites.<sup>[10–13]</sup> The major drawback of this process are also the high costs associated with the consumption of reductants.<sup>[7]</sup>

Direct catalytic decomposition of N<sub>2</sub>O without addition of reducing agents is an attractive and economical option to reduce N<sub>2</sub>O emission. Catalysts, including supported noble

metals, metal oxides, and perovskites, are active in direct catalytic N<sub>2</sub>O decomposition.<sup>[14–16]</sup> The commercial iron-zeolite catalysts perform quite well in the presence of other gases, such as O<sub>2</sub>, NO<sub>x</sub>, or H<sub>2</sub>O, even in the presence of CO<sub>2</sub> and SO<sub>2</sub>.<sup>[17]</sup> However, metal oxide catalysts suffer from oxygen inhibition, and a low reaction rate of the N<sub>2</sub>O decomposition is observed.

To avoid inhibition by adsorbed oxygen, the O<sub>2</sub> formed can be directly removed from the reaction zone by an oxygen-selective membrane. A novel perovskite membrane,<sup>[18–27]</sup> which also acts as the catalyst, has the composition BaCo<sub>x</sub>Fe<sub>y</sub>Zr<sub>1–x–y</sub>O<sub>3–δ</sub> (BCFZ) with hollow-fiber geometry.<sup>[18–21]</sup>

The basic concept is shown in the Figure 1: N<sub>2</sub>O catalytically decomposes on the perovskite membrane surface to N<sub>2</sub> and surface oxygen (O\*) according to Equation (1).



Afterwards, O\* is removed as oxygen ions (O<sup>2–</sup>) through the membrane, and local charge neutrality is maintained by counterdiffusion of electrons (e<sup>–</sup>). To ensure a sufficient driving force for the oxygen transport through the membrane, and thus rapid removal of oxygen, methane is fed to the permeate side of the membrane to consume the permeated oxygen by the partial oxidation of methane (POM) to synthesis gas according to CH<sub>4</sub> + O<sup>2–</sup> → CO + 2H<sub>2</sub> + 2e<sup>–</sup>. As a result, surface oxygen (O\*) can be quickly removed by the membrane once it is generated from N<sub>2</sub>O decomposition. Therefore, the average amount of adsorbed oxygen (O\*) is decreased on the catalyst surface, and a higher reaction rate of the N<sub>2</sub>O decomposition is obtained.

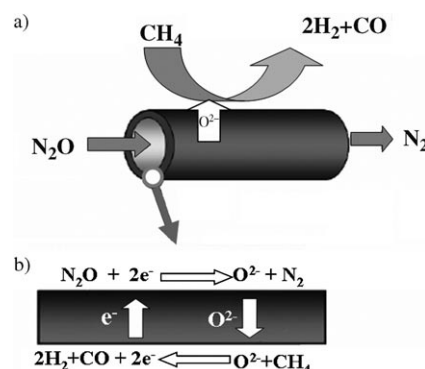


**Figure 1.** a) Mechanism of the direct decomposition of N<sub>2</sub>O to N<sub>2</sub> with in situ removal of the rate-inhibiting surface oxygen by a perovskite hollow fiber membrane. b) Details of the membrane reaction.

[\*] Prof. Dr. H. Wang  
School of Chemistry & Chemical Engineering  
South China University of Technology  
Wushan Road, Guangzhou 510640 (China)  
Fax: (+86) 208-711-0131  
E-mail: hhwang@scut.edu.cn  
Dr. S. Werth  
Uhde GmbH  
Friedrich-Uhde-Strasse 15, 44141 Dortmund (Germany)  
Fax: (+49) 212-6455872  
E-mail: steffen.werth@werthnetz.de  
H. Jiang, F. Liang, Prof. Dr. J. Caro  
Institute of Physical Chemistry and Electrochemistry  
Leibniz University of Hannover  
Callinstrasse 3–3A, 30167 Hannover (Germany)  
Fax: (+49) 511-762-19121  
E-mail: juergen.caro@pci.uni-hannover.de  
Dr. T. Schiestel  
Fraunhofer Institute of Interfacial Engineering and Biotechnology (IGB)  
Nobelstrasse 12, 70569 Stuttgart (Germany)

[\*\*] The authors gratefully acknowledge the financial support of the BMBF for project 03C0343A under the auspices of ConNeCat and H.W. thanks the NSFC (No.20706020) for financial support. The authors thank Prof. F. Kapteijn (TU Delft) and Dr. M. Schaefer (Uhde, Dortmund) for helpful discussions.

Supporting information for this article is available on the WWW under <http://dx.doi.org/10.1002/anie.200804582>.

To demonstrate this concept, we carried out experiments with and without oxygen removal using a BCFZ perovskite hollow fiber membrane. In the first set of experiments, N<sub>2</sub>O was fed to the core side and no sweep gas was applied at the shell side, so that none of the oxygen surface species produced by the decomposition of N<sub>2</sub>O were removed by permeation through the membrane (Supporting Information, Figure S1). The BCFZ membrane thus functions as a catalyst only.

The results of these investigations are shown in Figure 2a. The N<sub>2</sub>O decomposition increases with increasing temperature; however, the conversion is relatively low (< 30 % even

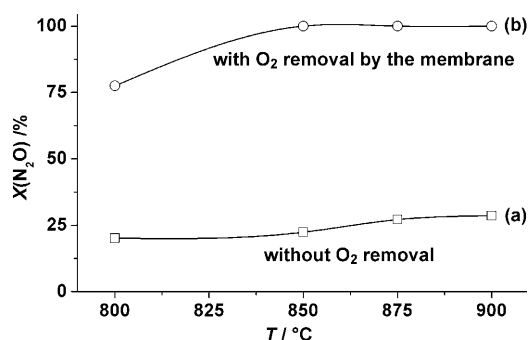


**Figure 2.** Conversion of N<sub>2</sub>O at different temperatures with or without oxygen removal by the membrane. Core side: 30 cm<sup>3</sup> min<sup>-1</sup> ( $F_{\text{N}_2\text{O}} = 6 \text{ cm}^3 \text{ min}^{-1}$ ,  $F_{\text{He}} = 24 \text{ cm}^3 \text{ min}^{-1}$ ). Shell side: a) no oxygen-consuming sweep gas applied, b) with methane as oxygen-consuming sweep gas, 40 cm<sup>3</sup> min<sup>-1</sup> ( $F_{\text{CH}_4} = 8 \text{ cm}^3 \text{ min}^{-1}$ ,  $F_{\text{Ne}} = 12 \text{ cm}^3 \text{ min}^{-1}$ ,  $F_{\text{H}_2\text{O}} = 20 \text{ cm}^3 \text{ min}^{-1}$ ). Membrane area: 0.86 cm<sup>2</sup>. Amount of nickel-based catalyst on shell side: 1.2 g.

at 900°C). The catalytic decomposition of N<sub>2</sub>O on the perovskite membrane surface proceeds mainly in two steps: 1) decomposition of N<sub>2</sub>O into N<sub>2</sub> and adsorbed surface oxygen (O\*) according to Equation (1), and 2) desorption of surface oxygen as O<sub>2</sub> to the gas phase according to Equation (2).



Equation (2), that is, the oxygen–oxygen recombination, is known to be the rate-limiting step in N<sub>2</sub>O decomposition.<sup>[28,29]</sup> As the surface oxygen O\* generated by the N<sub>2</sub>O decomposition occupies the surface active sites for the decomposition of N<sub>2</sub>O, only a low N<sub>2</sub>O conversion is obtained.

In the second set of experiments, methane was fed to the shell side (Supporting Information, Figure S1). In contrast to the poor conversion of the first set, in the second set, the N<sub>2</sub>O decomposition is significantly improved (Figure 2b). At a temperature of 850°C, N<sub>2</sub>O is already completely decomposed. The reason for this enhanced conversion is an increased removal of the adsorbed surface oxygen. In contrast to the first experiment, the adsorbed surface oxygen, along with desorption to the gas phase, can be also removed directly by the perovskite material functioning as a membrane. The active centers are thus less occupied by adsorbed oxygen on the catalyst surface and therefore the reaction rate is increased.

In the direct catalytic decomposition of N<sub>2</sub>O, most of the metal oxide catalysts cannot tolerate the coexistence of oxygen in the feed because the oxygen inhibits the N<sub>2</sub>O decomposition. However, oxygen as co-feed has no negative effect on the N<sub>2</sub>O decomposition in the membrane reactor. Table 1 shows the N<sub>2</sub>O conversion and oxygen concentration

**Table 1:** Oxygen concentration in the off-gas as a function of the oxygen concentration in the mixed N<sub>2</sub>O/O<sub>2</sub> feed gas at 100% N<sub>2</sub>O conversion.<sup>[a]</sup>

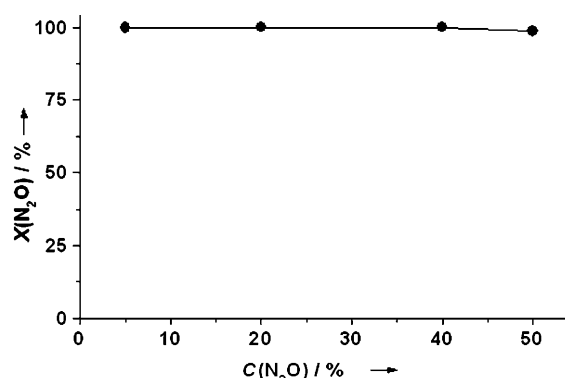
C(O <sub>2</sub> ) in the fed N <sub>2</sub> O of the core side [vol. %]	C(O <sub>2</sub> ) in the exit of the core side [vol. %]
0	0.011
5	0.014
7.5	0.019
15	0.022

[a] At 875°C. Core side: 30 cm<sup>3</sup> min<sup>-1</sup> ( $F_{\text{N}_2\text{O}} = 6 \text{ cm}^3 \text{ min}^{-1}$ ,  $F_{\text{O}_2} = 1.5\text{--}4.5 \text{ cm}^3 \text{ min}^{-1}$ ,  $F_{\text{He}} = \text{balance}$ ). Shell side: 40 cm<sup>3</sup> min<sup>-1</sup> ( $F_{\text{CH}_4} = 18 \text{ cm}^3 \text{ min}^{-1}$ ,  $F_{\text{H}_2\text{O}} = 22 \text{ cm}^3 \text{ min}^{-1}$ ). Membrane area: 0.86 cm<sup>2</sup>. Amount of nickel-based catalyst on shell side: 1.2 g.

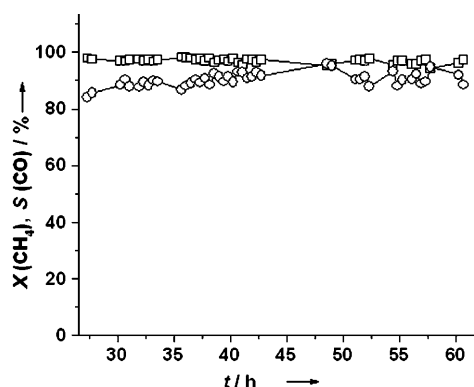
at the reactor outlet as a function of oxygen concentration in a mixed N<sub>2</sub>O/O<sub>2</sub> feed. A complete conversion of N<sub>2</sub>O is always achieved, which does not change with increasing oxygen concentration in the range studied in the feed, as both the co-fed and the produced oxygen are removed continuously by the membrane.

Figure 3 shows the influence of the N<sub>2</sub>O concentration on the N<sub>2</sub>O decomposition. Both low (5 %) and high (50 %) N<sub>2</sub>O concentrations can be effectively treated (conversion of N<sub>2</sub>O > 99.9 %) using the BCFZ membrane reactor.

The membrane approach presented herein involves the in situ removal of pure oxygen, which could then be utilized. An attractive option for the use of this oxygen is in the production of N<sub>2</sub>-free synthesis gas. In Figure 4, N<sub>2</sub>O in the core side was completely converted. Simultaneously, synthesis gas is obtained by partial oxidation of methane. Using suitable reaction conditions, a methane conversion of over 90 % and a CO selectivity of 90 % was achieved for at least 60 h of operation. The technology is more feasible when the concen-



**Figure 3.** Influence of the N<sub>2</sub>O concentration in the fed gas on the N<sub>2</sub>O conversion at 875°C. Core side: 30 cm<sup>3</sup> min<sup>-1</sup> ( $F_{\text{N}_2\text{O}} = 1.5\text{--}15 \text{ cm}^3 \text{ min}^{-1}$ ,  $F_{\text{He}} = \text{balance}$ ). Shell side: 40 cm<sup>3</sup> min<sup>-1</sup> ( $F_{\text{CH}_4} = 8 \text{ cm}^3 \text{ min}^{-1}$ ,  $F_{\text{Ne}} = 12 \text{ cm}^3 \text{ min}^{-1}$ ,  $F_{\text{H}_2\text{O}} = 20 \text{ cm}^3 \text{ min}^{-1}$ ). Membrane area: 0.86 cm<sup>2</sup>. Amount of nickel-based catalyst on shell side: 1.2 g.



**Figure 4.** Methane conversion  $X(\text{CH}_4)$  ( $\square$ ) and CO selectivity  $S(\text{CO})$  ( $\circ$ ) as a function of time on-stream at 875 °C with 100%  $\text{N}_2\text{O}$  conversion. Core side:  $30 \text{ cm}^3 \text{ min}^{-1}$  ( $F_{\text{N}_2\text{O}} = 6 \text{ cm}^3 \text{ min}^{-1}$ ,  $F_{\text{O}_2} = 1.5 \text{ cm}^3 \text{ min}^{-1}$ ,  $F_{\text{He}} = 22.5 \text{ cm}^3 \text{ min}^{-1}$ ). Shell side:  $40 \text{ cm}^3 \text{ min}^{-1}$  ( $F_{\text{CH}_4} = 23 \text{ cm}^3 \text{ min}^{-1}$ ,  $F_{\text{H}_2\text{O}} = 17 \text{ cm}^3 \text{ min}^{-1}$ ). Membrane area:  $0.86 \text{ cm}^2$ . Amount of nickel-based catalyst on shell side: 1.2 g.

trations of nitrous oxide in the off-gas are sufficient high, such as in adipic acid plants.

In conclusion, a perovskite membrane reactor is proposed for the  $\text{N}_2\text{O}$  abatement from exhaust gases. The ceramic membrane fulfills a double role: it catalyzes the decomposition of  $\text{N}_2\text{O}$  on the membrane surface, and it increases the reaction rate by overcoming the rate-limiting removal of surface oxygen, thus increasing the number of active surface sites required for the  $\text{N}_2\text{O}$  decomposition. A reducing agent has to be used; this agent, for example methane, can however be used for the production of  $\text{N}_2$ -free synthesis gas by partial oxidation using the removed oxygen from  $\text{N}_2\text{O}$  decomposition as an oxidant.

The work presented herein is the new concept to enhance the reaction rate of heterogeneous catalytic processes, in which the recombination and/or desorption of one of the reaction products is the rate-limiting step. Using a semi-permeable membrane, which facilitates in situ removal of an inhibiting species on a catalyst or catalyst support, helps to effectively reduce the surface concentration of the inhibiting species and therefore increases the reaction rate.

## Experimental Section

The dense BCFZ perovskite hollow-fiber membranes were manufactured by phase inversion spinning followed by sintering.<sup>[18–21]</sup> Figure S1 (Supporting Information) shows diagrams of the membrane reactor used in this study. Two ends of the hollow fiber were coated by commercially available gold paste. After sintering at 950 °C, a dense gold film, which is not permeable to oxygen, was obtained. Such gold-coated hollow fibers can be sealed by silicon rubber rings and the uncoated part of the fiber (3.0 cm) that is permeable to oxygen can be kept in the middle of the oven, ensuring isothermal conditions. A mixture of  $\text{N}_2\text{O}$  and helium was fed to the core side and a mixture of  $\text{CH}_4$  and helium was fed to the shell side. A nickel-based steam reforming catalyst (Süd-Chemie AG) was packed around and behind the hollow fiber membrane. To avoid coke formation on the catalyst,  $\text{H}_2\text{O}$  was also fed to the shell side. The  $\text{H}_2\text{O}$  flow rate was controlled by a liquid mass flow controller (Bronkhorst) and completely evaporated at 180 °C before it was fed to the reactor. All gas lines to the reactor and the gas chromatograph were heated to 180 °C to

avoid condensation. The concentrations of the gases at the exit of the reactor were determined by on-line gas chromatography (Agilent 6890 with a carboxen 1000 column, which was periodically switched from the core-side to the shell-side of the membrane to measure the gas compositions on both sides of the membrane). The  $\text{CH}_4$  conversion  $X(\text{CH}_4)$ , the CO selectivity  $S(\text{CO})$  and the  $\text{N}_2\text{O}$  conversion were calculated as shown in Equations (3)–(5).

$$X(\text{CH}_4) = \left(1 - \frac{F(\text{CH}_4, \text{out})}{F(\text{CH}_4, \text{in})}\right) \times 100\% \quad (3)$$

$$S(\text{CO}) = \frac{F(\text{CO}, \text{out})}{F(\text{CH}_4, \text{in}) - F(\text{CH}_4, \text{out})} \times 100\% \quad (4)$$

$$X(\text{N}_2\text{O}) = \left(1 - \frac{F(\text{N}_2\text{O}, \text{out})}{F(\text{N}_2\text{O}, \text{in})}\right) \times 100\% \quad (5)$$

In these equations,  $F(i)$  is the flow rate of species  $i$  on the shell or core side of the hollow fiber membrane.

Received: September 17, 2008

Revised: November 16, 2008

Published online: January 23, 2009

**Keywords:** membrane reactors ·  $\text{N}_2\text{O}$  decomposition · partial oxidation of methane · perovskite · syngas

- [1] R. E. Dickinson, R. J. Cicerone, *Nature* **1986**, *319*, 109.
- [2] M. J. Prather, *Science* **1998**, *279*, 1339.
- [3] S. J. Hall, P. A. Matson, *Nature* **1999**, *400*, 152.
- [4] J. E. Dore, B. N. Popp, D. M. Karl, F. J. Sansone, *Nature* **1998**, *396*, 63.
- [5] T. Nobukawa, K. Sugawara, K. Okumura, K. Tomishige, K. Kunimori, *Appl. Catal. B* **2007**, *70*, 342.
- [6] F. Kapteijn, J. Rodriguez-Mirasol, J. A. Moulijn, *Appl. Catal. B* **1996**, *9*, 25.
- [7] J. Pérez-Ramírez, F. Kapteijn, K. Schöffel, J. A. Moulijn, *Appl. Catal. B* **2003**, *44*, 117.
- [8] M. Schwefer, R. Maurer, M. Groves in *Proceedings of the International Conference and Exhibition on Nitrogen*, Vienna, 12–14 March **2000**, pp. 60–81.
- [9] C. Pophal, T. Yogo, K. Yamada, K. Segawa, *Appl. Catal. B* **1998**, *16*, 177.
- [10] M. Kögel, R. Moenning, W. Schwieger, A. Tissler, T. Turek, *J. Catal.* **1999**, *182*, 470.
- [11] Z. S. Rak, M. J. F. M. Verhaak, B. Bos, G. Centi (ECN), WO99/49954, **1999**.
- [12] M. Schwefer, R. Mauer, T. Turek, M. Kögel (Krupp Uhde), WO0151182, **2001**.
- [13] J. Pérez-Ramírez, F. Kapteijn, G. Mul, J. A. Moulijn, *Chem. Commun.* **2001**, 693.
- [14] G. Centi, A. Galli, B. Montanari, S. Perathoner, A. Vaccari, *Catal. Today* **1997**, *35*, 113.
- [15] N. Russo, D. Fina, G. Saracco, V. Specchia, *Catal. Today* **2007**, *119*, 228.
- [16] N. Gunasekaran, S. Rajadurai, J. J. Carberry, *Catal. Lett.* **1995**, *35*, 373.
- [17] J. Pérez-Ramírez, F. Kapteijn, G. Mul, J. A. Moulijn, *Appl. Catal. B* **2002**, *35*, 227.
- [18] T. Schiestel, M. Kilgus, S. Peter, K. J. Caspary, H. H. Wang, J. Caro, *J. Membr. Sci.* **2005**, *258*, 1.
- [19] H. H. Wang, S. Werth, T. Schiestel, J. Caro, *Angew. Chem.* **2005**, *117*, 7066; *Angew. Chem. Int. Ed.* **2005**, *44*, 6906.
- [20] H. H. Wang, P. Kölsch, T. Schiestel, C. Tablet, S. Werth, J. Caro, *J. Membr. Sci.* **2006**, *284*, 5.

- [21] C. Hamel, A. Seidel-Morgenstern, T. Schiestel, S. Werth, H. H. Wang, C. Tablet, J. Caro, *AIChE J.* **2006**, *52*, 3118.
  - [22] J. Y. Ren, Y. Q. Fan, F. N. Egolfopoulos, T. T. Tsotsis, *Chem. Eng. Sci.* **2003**, *58*, 1043.
  - [23] R. Merkle, J. Maier, H. J. M. Bouwmeester, *Angew. Chem.* **2004**, *116*, 5179; *Angew. Chem. Int. Ed.* **2004**, *43*, 5069.
  - [24] J. Pérez-Ramírez, B. Vigeland, *Angew. Chem.* **2005**, *117*, 1136; *Angew. Chem. Int. Ed.* **2005**, *44*, 1112.
  - [25] Z. P. Shao, W. S. Yang, Y. Cong, H. Dong, J. H. Tong, G. X. Xiong, *J. Membr. Sci.* **2000**, *172*, 177.
  - [26] C. Chen, S. J. Feng, S. Ran, D. C. Zhu, W. Liu, H. J. M. Bouwmeester, *Angew. Chem.* **2003**, *115*, 5354; *Angew. Chem. Int. Ed.* **2003**, *42*, 5196.
  - [27] F. T. Akin, Y. S. Lin, *AIChE J.* **2002**, *48*, 2298.
  - [28] D. A. Bulushev, L. Kiwi-Minsker, A. Renken, *J. Catal.* **2004**, *222*, 389.
  - [29] S. Bennici, A. Gervasini, *Appl. Catal. B* **2006**, *62*, 336.
-